IEEE Access
Multidisciplinary | Rapid Review | Open Access Journal

Received November 16, 2017, accepted January 16, 2018, date of publication January 23, 2018, date of current version March 12, 2018.

Digital Object Identifier 10.1109/ACCESS.2018.2797087

Microwave Photonic Downconversion With Improved Conversion Efficiency and SFDR

FADIL PALOI[1], SHYQYRI HAXHA[1,2], (Senior Member, IEEE), TAIMUR N MIRZA[1,2], AND MOHAMMED SHAH ALOM[1,2]

[1]Department of Computer Science and Technologies, University of Bedfordshire, Luton LU1 3JU, U.K.
[2]Department of Electronic Engineering Egham, Royal Holloway, University of London, Egham TW20 0EX, U.K.

Corresponding author: Shyqyri Haxha (shyqyri.haxha@rhul.ac.uk)

ABSTRACT In this paper, we report a novel approach of microwave frequency downconversion with improved conversion efficiency and high dynamic range, using two different configuration schemes. The first proposed scheme is designed by using a dual-parallel dual-drive Mach–Zehnder modulator and the second one using dual-parallel dual-phase modulator. The radio frequency (RF) message signal and the local oscillator (LO) signal are feeding these two parallel connected modulators. By using a tight control of the system parameters, we have reported an effective optical carrier suppression, resulting in high conversion efficiency. We show that when the link is amplified, the relation between m_{LO} and m_{RF} plays a vital role and gives a high value of conversion efficiency, where key parameters lead to the LO and RF modulators modulation index. The conversion efficiency is improved by 5.72 dBm, compared with previously published work using DP-MZM, and 28.4 dBm, compared with the cascaded connected modulator. An experimental demonstration of a proof of concept is also carried out where the intermediate frequency to noise ratio of 69.5 dB is reported.

INDEX TERMS Microwave photonic downconversion, dual parallel phase modulation, optical carrier suppression.

I. INTRODUCTION

The photonic microwave is a powerful paradigm for signal processing due to low transmission losses, high isolation, wide bandwidth and immune to the electromagnetic interference. For many applications, the crucial task when designing a RoF link is downconverting the high-frequency microwave signal to a lower intermediate frequency (IF), with the least possible losses, with a reduction of the bandwidth requirement, and an enhancement of the DR [1].

To recover the high-frequency signal, and digitise with high resolution, it is necessary to downconvert signal to a lower intermediate frequency (IF), which can be easily matched. A variety of microwave photonic downconversion structures have been reported, employing two or more modulators connected at the various configuration [2]. Each configuration has advantages and disadvantages. The most common is downconversion with conventional electrical mixing. Following with the optical downconversion using heterodyne mixing of two coherent optical carriers at the photodetector (PD), where higher frequency signals are downconverted to the low-frequency signals as a result, the system suffers from high optical power [3], [4]. Nevertheless, the cascade electro-optic modulator connection allows modulators to be located at the different position but on the other hand, they suffer from high nonlinear properties, resulting in very low conversion efficiency [5]–[7]. Furthermore, the parallel connection of two or more modulators with RF and LO signal connected at the base station, have provided higher downconversion efficiency, but still, there is space to improve the system's efficiency and DR [8]. The previously reported techniques are suffering from very low conversion efficiency by increasing the system's nonlinearities and reducing the system's bandwidth [9].

In this paper, by applying a stringent control on the system parameters, we present a configuration obtaining high conversion efficiency, wide bandwidth, and stable output signal. We are proposing schemes with improved conversion efficiency and spurious free dynamic range photonic microwave downconversion, using DP-DDMZM, first driven by a stronger LO and second driven by an RF message signal.

We have simulated our proposed model and benchmarked with experimental work published by [5] and [10] (as shown

TABLE 1. Integrated DP-DDMZM based photonic mixer performance compared to the [10], DP-MZM.

Operating Point	Compared DPMZM	Proposed DPDPM
Conv. Efficiency	7.8 dB	13.52 dB
Noise Figure	23.5 dB	23.29 dB
SFDR	115.6dB-Hz$^{2/3}$	121.15dB-Hz$^{2/3}$

in Table 1). High conversion efficiency has been achieved by suppressing the optical carrier at the DP-DDMZM, configured as phase modulators, or DP-DPhM, enabling high amplitude of the LO and RF sidebands into the receiver, achieving high conversion efficiency, high Spurious Free Dynamic Range (SFDR) and the capability to work over a wide frequency range. In the first proposed configuration, with DP-DDMZM working as a full phase modulator, by using a tight control on the Gallium Arsenide (GaAs) MZMs parameters, and controlling the electrical signal at both electrodes [11]–[13], the residual carrier has been effectively suppressed. The second method, configured with DP-DPhM [14] is considered with the adequate phase difference between each sets of dual phase modulator, achieving high IF amplitude with the low spur and high SFDR. Furthermore, the simulation design approach alongside the theoretical analysis of the proposed structure, should allow the optimisation of the microwave photonic downconversion performance, for the benefits of photonic signal transmission.

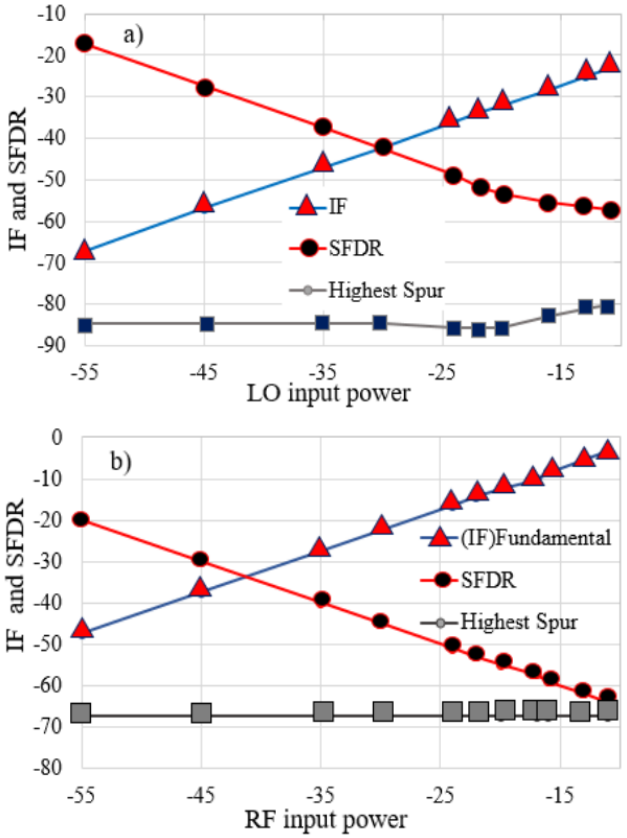

FIGURE 1. IF and Dynamic Range in function of (a) LO input power for the DP-DDMZM and (b) RF input power for the DP-DDMZM.

II. METHODOLOGY

In our proposed configuration, we have used two different configuration schemes. The first scheme is designed by using DP-DDMZM configured as a phase modulator. The second scheme is designed by replacing both dual drive parallel modulators of the first scheme with Dual Parallel Phase Modulators (DPDPM) [14], [15]. At both configuration schemes, the first modulator is driven by a stronger LO and the second by an RF message signal, generating downconverted IF signal.

A thought-provoking approach within this system configuration is the way shifting and biasing is utilised to downconvert the signal frequency [4], [16]. We have deployed VPI simulation software packages to implement the analytical model and to analyse the proposed system performance [17].

Initially, we studied a few action points, investigating the behaviour of the harmonics in function of RF and LO input power, utilised in the conventional DP-MZM configuration, as illustrated in the Fig. 1 (a, b). The LO and RF input power significantly affects the system's performance, particularly impacting the harmonic distortion and resulting in adequate SFDR.

At the same structure, it is impossible to obtain constant conversion efficiency given that input RF power is dependent on the RF modulation index.

The optimisation of the proposed RoF system is performed by applying techniques of carrier suppression. Optical carrier suppression in the DP-DDMZM photonic mixer can be achieved by controlling the modulator's bias voltage and adequate time delay [16]. In our proposed structure, by applying the technique of carrier suppression we keep the output spectrum simple, not putting high optical power into the receiver which adds to the noise.

Another efficient technique utilised in dual parallel configurations is biasing the system at the minimum transmission point (mTP), in the push-pull operating mode [4]. The DP-DDMZM forms push-pull configuration mode when the LO signal ($V_{LO}cos\,\omega_{LO}t$), at the first modulator or an RF message signal ($V_{RF}cos\,\omega_{RF}t$) at the second modulator into two equal branches ($V_{11}(t)$ and $V_{12}(t)$), is defined as cosine-wave and inverse cosine-wave signal.

The DP-DDMZM operates at the minimum Transmission Point (mTP) when LO or RF message signal together with DC switching voltages of $V\pi = V_{DC} = V_{b11} - V_{b12} = \pi = 5.6$[V], for both branches ($V_{b11} = 2.8$[V] *and* $V_{b12} = -2.8$[V]) is applied, resulting in low gain, low spur product, and high SFDR, as shown in table 2, [16]. Other efficient techniques, achieving carrier suppression in the DP-DDMZM configuration is biasing the modulator at the quadrature transmission point, in the push-pull operation mode. The DP-DDMZM can operate at the Quadrature Transmission Point (QTP) when the LO or RF message signal together

TABLE 2. Integrated DP-DDMZM based photonic mixer performance compared to the various DP-MZM based photonic mixer.

Modulators		Operating Point	SFDR with EDFA	SFDR no EDFA
DPMZM (IM)	Conventional	mTP	50.5 dBm	52.94 dBm
DPMZM (IM)	Conventional	QTP	47.1 dBm	28.92 dBm
DPMZM (IM)	Conventional	Peak (MTP)	17 dBm	18.81 dBm
DPMZM (IM)	Based on Ref. [5]	QTP	58.9 dBm	N/A
DPMZM (PM)	Based on Ref. [5]	Peak (MTP)	67 dBm	N/A
DPMZM (PM)	Based on Ref. [5]	mTP	67 dBm	N/A
DPMZM (PM)	Proposed Configure.	QTP	69.2 dBm	N/A
Phase Modulator	Proposed Configure.	Any	71.6 dBm	N/A

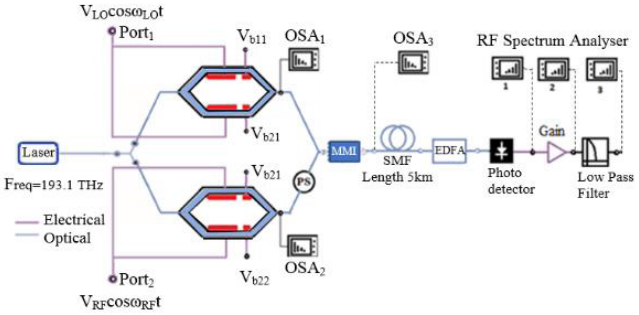

FIGURE 2. Proposed DDMZM based microwave photonic downconverter, formed by two Parallel MZM and optical phase shift. at the push-pull operating mode, SSMF, EDFA, Optical receiver (RX).

with DC switching voltage $V\pi = V_{bias} = V_{b21} - V_{b22} = \pi/2$=2.8[V] for both branches ($V_{b21} = 1.4$[V] *and* $V_{b22} = -1.4$[V]) is applied, results in a high gain and minimised even order distortion, as shown in table 2.

III. DOWNCONVERSION DESIGN

This configuration is based on the DP-DDMZM and optical shift with two-tone frequencies, for the first modulator driven by the strong LO signal at the frequency of 15GHz and second parallel connected modulator driven by the RF message signal at the frequency of 14.92 GHz. The optical source used is CWL, with narrow linewidth at the reference frequency of 193.4THz. The incoming signal from each modulator is split equally between each DDMZM. Each arm of the DDMZM is driven by the modulating voltage, as shown in the Fig.2, [15].

The second proposed scheme is constructed by two DP-DPhMs. This configuration structure is based on the phase deviation, which represents the difference between the phase angle of the modulated wave and the phase angle of the unmodulated carrier [18]. The phase deviation between each sets of dual phase modulator is set at 135°. We have simulated both our proposed models and benchmarked them with experimental work published by [5] and [10], as shown in table 2. Our simulation results show that the carrier is the dominant output optical component with the highest consumed power. For the parallel modulator connection, the carrier is not required at the frequency downconversion. The average power travelling to the receiver can be reduced by decreasing input power, such as the carrier power. By optical carrier suppression in the modulated link, the modulated depth will increase and will result in an increase of SFDR. The high conversion efficiency can also be obtained by carrier suppression, subsequently, we should find the means to suppress the carrier to the maximum extent.

The parallel connection of phase modulators can be used to convert the phase modulated signal into intensity, and suppress or cancel the carrier [4], [14], [19]. The residual carrier can be cancelled by a combination of differential signal detection of both modulators. This can be achieved by the phase shifting, and at some configuration by proper biasing. One means of carrier suppression is the inverse biasing of both DP-DDMZM. The other means is by 180° shifting of DP-DDMZM.

In the proposed configuration, shown in Fig. 2, to achieve carrier suppression, we have used a mTP of biasing, with inverse biasing of both modulators, where the phase shifting (PS) is not required.

At the mTP or Null Operating Point (NOP) each branch of the DDMZM is biased at $V_{bias1} = 2.8$[V] and $V_{bias2} = -2.8$[V], where $V_{DC} = V_{\pi} = 5.6$[V], [16].

The next method employed is the QTP of biasing. The QTP can be achieved when modulators are biased with $V_{bias1} = 1.4$V, at the upper branch, and with $V_{bias2} = -1.4$V at the lower branch, where $V_{DC} = V\pi/2 = 2.8$[V].

Another option to achieve carrier suppression is Maximum Transmission Point (MTP), where each modulator should be biased with $V_{bias1} = 5.6$[V] and $V_{bias2} = 5.6$[V], where $V_{DC} = 0$[V], and by 180° shifting of parent modulator.

IV. DOWNCONVERSION THEORY

Initially, our starting point is conversion efficiency, which is a ratio between the output power generated as IF and input power at the second modulator driven by the RF message signal [19]. By amplifying the link, the LO and RF sidebands will rise much faster, and noise generated during the amplification such as ASE can be amplified too, and should be optically filtered.

The analytical calculation shows that conversion efficiency is significantly related to the modulator's modulation indexes. By employing two DD-MZMs or two DP-DPhMs, the instantaneous value of the modulated signal is applied to the upper and lower branch of each modulator. Both branches modulating voltages can be expressed as two invers cosines signals, $V_{11}cos\omega_{RF}$ *and* $-V_{12}cos\omega_{RF}$, [14].

The modulating voltage together with the bias voltage applied to each arm of the top MZM_1, for the push-pull configuration, can be expressed as follows, as shown

in Fig. 2 [6] [15]:

$$\mathrm{V}_{11}(t) = \mathrm{V}_{11}\cos\omega_{LO}t + V_\pi/2 \tag{1}$$

$$\Phi_{11}(t) = \pi\frac{\mathrm{V}_{11}(t)}{V_\pi} = \pi\frac{\mathrm{V}_{11}}{V_\pi}\cos\omega_{LO}t + \pi\frac{\mathrm{V}_{\pi\mathrm{DC}}}{2V_\pi} \tag{2}$$

$$\mathrm{V}_{12}(t) = \mathrm{V}_{12}\cos(\omega_{LO}t + \pi) \tag{3}$$

$$\Phi_{12}(t) = \pi\frac{\mathrm{V}_{12}(t)}{V_\pi} = -\pi\frac{\mathrm{V}_{12}}{V_\pi}\cos\omega_{LO}t - \pi\frac{\mathrm{V}_{\pi\mathrm{DC}}}{2V_\pi} \tag{4}$$

$$\mathrm{E}_{\mathrm{MZM}}(t) = \mathrm{E}_0 e^{j\omega_0 t}\left\{\sqrt{r_1 r_2}e^{j\Phi_{11}(t)} + \sqrt{(1-r_1)(1-r_2)}e^{j\Phi_{12}(t)}\right\} \tag{5}$$

The optical power distributed by the laser will reach the input connection of the DD-MZM with the broadcasting coefficient of $r_1 = r_2$, which is the ideal power splitting ratio. We will present a calculation of the electrical field for the first double phase modulators driven by an LO message signal [20]:

$$\mathrm{E}_{\mathrm{MZM1}}(t) = \frac{\mathrm{E}_0}{2}e^{j\omega_0 t}\left\{e^{j\Phi_{11}(t)} + e^{j\Phi_{12}(t)}\right\} \tag{6}$$

Based on the Push-Pull configuration, where: $V_{11}(t) = -V_{12}(t)$.

$$V_{Bias} = V_{dc11} - V_{dc12} = \frac{V_\pi}{2} - (-\frac{V_\pi}{2}) = V_\pi;$$

then

$$= \mathrm{E}_0 e^{j\omega_0 t}\left\{\begin{array}{l}\cos\left(\pi\dfrac{V_{dc11}-V_{dc12}}{2V_\pi} + \pi\dfrac{V_{11}(t)-V_{12}(t)}{2V_\pi}\right)\\ e^{j[\pi\frac{V_{dc11}+V_{dc12}}{2V_\pi} + \pi\frac{V_{11}(t)+V_{12}(t)}{2V_\pi}]}\end{array}\right\} \tag{7}$$

$$= \mathrm{E}_0 e^{j\omega_0 t}\left\{\begin{array}{l}\cos\left(\pi\dfrac{V_{dc11}-V_{dc12}}{2V_\pi} + \pi\dfrac{V_{11}(t)-V_{12}(t)}{2V_\pi}\right)\\ e^{j[\pi\frac{0}{2V_\pi} + \pi\frac{0}{2V_\pi}]}\end{array}\right\}$$

$$\mathrm{E}_{\mathrm{MZM1}}(t) = \mathrm{E}_0 e^{j\omega_0 t}\left\{\cos\left(\frac{\pi}{2} + \pi\frac{2V_{p-p}}{2V_\pi}\cos\omega_{LO}t\right)\right\}$$

$$= \mathrm{E}_0 e^{j\omega_0 t}\left\{\begin{array}{l}\cos\dfrac{\pi}{2} + \cos\left(\pi\dfrac{V_{p-p}}{V_\pi}\cos\omega_{LO}t\right)\\ -\sin\dfrac{\pi}{2} + \sin\left(\pi\dfrac{V_{p-p}}{V_\pi}\cos\omega_{LO}t\right)\end{array}\right\}$$

$$m_{LO} = \pi\frac{V_{p-p}}{V_\pi} \tag{8}$$

Because each DDMZM photonic mixer is configured at the push-pull operation mode, and as seen from the derived Eq.7, the modulation index is twice that of the single drive. To the dual-drive push-pull configuration, the modulator's switching voltage is half of the single drive, [10]:

$$\mathrm{E}_{\mathrm{MZM1}}(t) = \mathrm{E}_0 e^{j\omega_0 t}\left\{-\sin\frac{\pi}{2}\cdot\sin(m_{LO}\cos\omega_{LO}t)\right\}$$

$$\mathrm{E}_{\mathrm{MZM1}}(t) = \mathrm{E}_0(\cos\omega_0 t + j\sin\omega_0 t)\{-\sin(m_{LO}\cos\omega_{LO}t)\}$$

By the inverse biasing of both modulators, or in the ideal condition when both modulators are shifted by 180° at the push pull configuration, the carrier is canceled. The equation will then take form as

$$\mathrm{E}_{\mathrm{MZM1}}(t) = \mathrm{E}_0\cdot\left\{\begin{array}{l}-\cos\omega_0 t\cdot\sin(m_{LO}\cos\omega_{LO}t)\\ -j\sin\omega_0 t\cdot\sin(m_{LO}\cos\omega_{LO}t)\end{array}\right\} \tag{9}$$

The equation can be solved by using the Bessel function identities, after Jacoby-Anger expansion, the output optic field for the top MZM_1 can be written as follows:

$$\mathrm{E}_{\mathrm{MZM1}}(t) = -\mathrm{E}_0\{2J_1(m_{LO})\cos\omega_0 t\cdot\cos\omega_{LO}t\}$$

$$\mathrm{E}_{\mathrm{MZM1}}(t) = -\mathrm{E}_0 J_1(m_{LO})\left\{\begin{array}{l}[\cos(\omega_0 t + \omega_{LO}t)\\ +\cos(\omega_0 t - \omega_{LO}t)]\end{array}\right\} \tag{10}$$

As can be seen from Eq. (10), the output of the first modulator's optical intensity depends on the LO modulation index, where both sidebands have the same amplitude:

$$m_{LO} = \pi\frac{V_{LO}}{V_\pi}. \tag{11}$$

The value of the reference LO modulation index used for the first modulator is $\mathrm{m_{LO}} = 0.22$, and the peak-peak voltages inserted at the first double phase modulators driven by the LO signal can be calculated from the same LO modulation index:

$$V_{LO} = \frac{m_{LO}\cdot V_\pi}{\pi} = \frac{0.22\cdot 5.6}{\pi} = 0.392[V] \tag{12}$$

The achieved $\mathrm{V_{LO}}$ voltage is used to calculate LO input power:

$$P_{LO} = \frac{\left(\frac{V_{LO}}{\sqrt{2}}\right)^2}{R} = \frac{(0.392)^2}{2\cdot 50} = 1,5378\cdot 10^{-3}[W]$$

$$P_{LO} = 1.868[dBm] \tag{13}$$

At the LO signal generator Fig. 2, we enter the achieved LO power:

We pursue a similar calculation for the second double phase modulator, driven by RF message signal, where electrical field will take form as:

$$\mathrm{E}_{\mathrm{MZM2}}(t) = \mathrm{E}_0 e^{j\omega_0 t}\left\{\begin{array}{l}\cos\left(\pi\dfrac{V_{dc21}-V_{dc22}}{2V_\pi} + \pi\dfrac{V_{21}(t)-V_{22}(t)}{2V_\pi}\right)\\ e^{j[\pi\frac{V_{dc21}+V_{dc22}}{2V_\pi} + \pi\frac{V_{21}(t)+V_{22}(t)}{2V_\pi}]}\end{array}\right\} \tag{14}$$

$$= \mathrm{E}_0\cdot\left\{\begin{array}{l}-\cos\omega_0 t\cdot\sin(m_{RF}\cdot\cos\omega_{RF}t)\\ -j\sin\omega_0 t\cdot\sin(m_{RF}\cdot\cos\omega_{RF}t)\end{array}\right\}\cdot e^{j\pi}$$

$$\mathrm{E}_{\mathrm{MZM2}}(t) = \mathrm{E}_0\{2J_1(m_{RF})\cos\omega_0 t\cdot\cos\omega_{RF}t\}$$

$$\mathrm{E}_{\mathrm{MZM2}}(t) = \mathrm{E}_0 J_1(m_{RF})\left\{\begin{array}{l}[\cos(\omega_0 t + \omega_{RF}t)\\ +\cos(\omega_0 t - \omega_{RF}t)]\end{array}\right\} \tag{15}$$

$$m_{RF} = \pi\frac{V_{RF}}{V_\pi} \tag{16}$$

Next, form the RFs modulation index value of $m_{RF} = 0.023$, and switching voltage of $V\pi = 5.6$ [V], we calculate the voltage entering the second modulator, driven by RF information signals:

$$V_{RF} = \frac{m_{RF} \cdot V_{\pi}}{\pi} = \frac{0.023 \cdot 5.6}{\pi} = 0.0403[V] \quad (17)$$

From the second modulator, the achieved V_{RF} voltage is utilised to calculate RF input power driven by the RF message signal:

$$P_{RF} = \frac{\left(\frac{V_{RF}}{\sqrt{2}}\right)^2}{R} = \frac{(0.0403)^2}{2 \cdot 50} = 16.21 \cdot 10^{-6}[W]$$
$$P_{RF} = -17.8[dBm] \quad (18)$$

At the LO signal generator we enter the achieved LO power to generate IF signal amplitude, and subsequently to calculate the conversion efficiency [19]:

$$\begin{aligned} &E_{DD\text{-}DPMZM}(t) \\ &= E_{MZM1}(t) + E_{MZM2}(t) \\ &= -E_0 \{2J_1(m_{LO}) \cos \omega_0 t \cdot \cos \omega_{LO} t\} \\ &\quad + E_0 \{2J_1(m_{RF}) \cos \omega_0 t \cdot \cos \omega_{RF} t\} \\ &= 2E_0 \cdot \cos \omega_0 t \left\{ \begin{matrix} J_1(m_{RF}) \cdot \cos \omega_{RF} t \\ -J_1(m_{LO}) \cdot \cos \omega_{LO} t \end{matrix} \right\} \end{aligned} \quad (19)$$

The average power entering the receiver is [10]

$$P_{avg} = P^*_{IN} G^*_{EDFA} \alpha \left\{ J_1(m_{LO})^2 + (\frac{m_{RF}}{2})^2 \right\} \quad (20)$$

The average power used in the system link can be decreased by reducing the input power which includes the carrier power (input power), link amplification and losses during modulation.

In the first proposed configuration, with DP-DDMZM working as a phase modulator Fig. 2, with tight control on the system modulation such as minimising the electrical signal difference between both electrodes, the residual carrier at the DP-DDMZM can be effectively suppressed [11]–[13].

The second configuration with DP-DPhM is characterised with the phase difference of 135° between each set of the dual phase modulator. This phase deviation represents the phase angle between the modulated wave and the phase angle of the unmodulated carrier [9], [14]. The responsivity of a photodiode is defined as a ratio between photodiodes photocurrent and incident light power, and is a measure of the sensitivity to the light [21]:

$$\Re = \frac{I_{IF}}{P_{AV}} \quad (21)$$

From this equation and adding some of the losses we can derive the intermediate current [10]

$$I_{IF} = \Re * P_{IN} * G_{EDFA} * \alpha \quad (22)$$

The receiver's input power is dependent on the optical input power P_{IN}, on the gain added to the system by the EDFA (G_{EDFA}), on losses, and on the photodiode's responsivity $\Re$. Given that the optical carrier is suppressed, or one can say cancelled, most of the power is added to the sideband, then based on Eq. (20), a relation between the m_{LO} and m_{RF} will give us the value of the average power.

Since LO modulation index m_{LO} is much larger than RF modulation index m_{RF}, the increase in the RF modulation index influences the EDFA and photodetector to saturate. To avoid this situation, the difference between LO and RF modulation indexes must be larger. It was also noticed that the conversion efficiency increases much faster when an amplified optical signal is kept at or around 0 (dBm) of a photodiode input power [10]:

$$J_1(m_{LO})^2 \gg (\frac{m_{RF}}{2})^2 \quad (23)$$

Based on the powers equation (Gain) [5]; $P = G = RI^2$

$$G = R_{IN} \cdot \Re^2 \cdot P^2_{IN} \cdot G^2_{EDFA} \cdot J_1(m_{LO})^2 \cdot (\frac{\pi}{V_{\pi}})^2 \cdot R^2_{OUT} \quad (24)$$

Where R_{IN} is the modulator's input resistance and R_{out} is the photodetector's load resistance. From these equations, it is evident that a very small modulation index will make changes in the average output optical power. When RF information signal increases, at some level it will exceed the photodiode's power handling capability to some conventional receivers.

To avoid power congestion of the photodiode, we must design relations between LO and RF modulation indexes [8], [10]:

$$m_{LO} \geq m_{RF} \quad (25)$$

To achieve high conversion efficiency, the LO modulation index should always be greater than the RF modulation index. This has also been verified by using VPI simulation software [17].

V. SIMULATION RESULTS

The system parameter values, used in the proposed system configuration are: Responsivity $\tilde{R}$=0.8 [A/W], the initial optical power into each DDMZM is $P_{in} = 25$ [mW], insertion losses of $\alpha = 4$ [dB], modulation input resistance $R_{in} = 50$ [Ω], and photodiode load resistance $R_{out} = 50$ [Ω]. The half wave switching voltages is set to the value of $V_{\pi} = 5.6$ [V], with modulation voltages of both branches set to the value of $V_{LO(upper)} = 2.8$ [V] and $V_{LO(lower)} = 2.8$ [V].

The generated 80 [MHz] output electrical signal (IF) of DP-DDMZM is based on a photonic mixer for a much larger LO modulation index m_{LO} than RF modulation index m_{RF}, at the RF frequency of 14.92 [GHz] and LO frequency of 15 [GHz]. The conversion efficiency is the difference between the message information signal amplitude and the achieved intermediate signal amplitude [18]. For the first modulator at the modulation index of $m_{LO} = 0.22$, calculated peak-peak voltage and power are; $V_{LO} = 0.392$ [V] and $P_{LO} = 1.868$ [dBm], Eq. (12, 13). For the second modulator

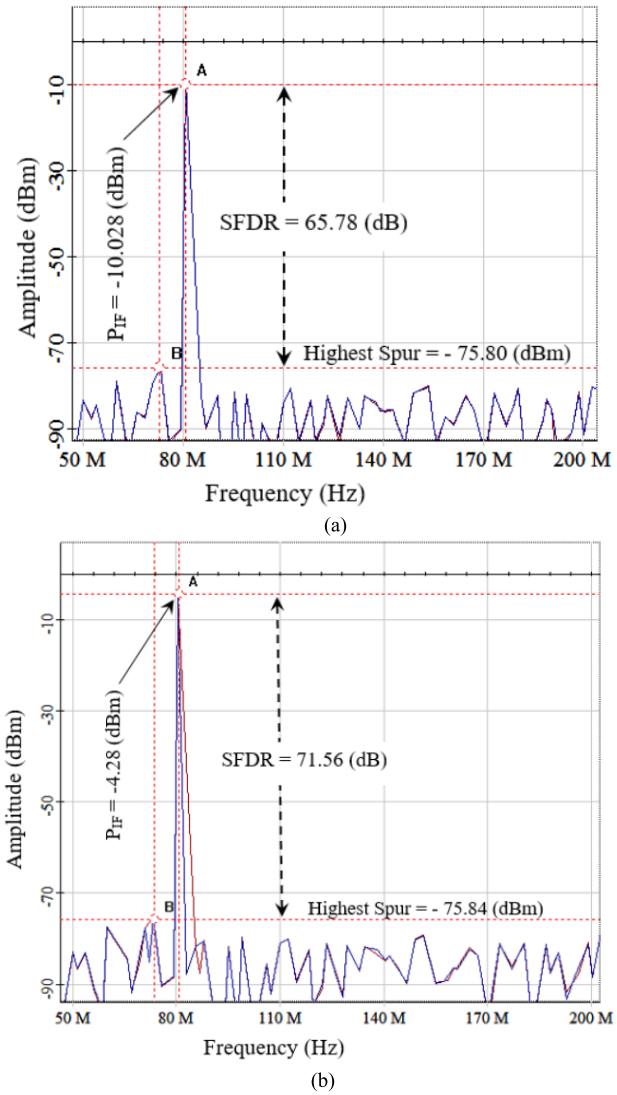

FIGURE 3. (a) Simulated output downconverted electrical spectrum (IF) of integrated DP-MZM, for the configuration, [10]. (b) Measured output downconverted electrical spectrum (IF) of integrated DP-MZM based photonic mixer, for the proposed configuration.

at the modulation index of $m_{RF} = 0.023$, calculated peak-peak voltage and power are $V_{RF} = 0.0403$ [V]and $P_{RF} = -17.8$ [dBm], Eq. (17, 18).

When we enter the above results in the system simulation for the configuration at [10], we achieve an intermediate signal power amplitude of $P_{IF} = -10$[dBm], with the low spur of 75.80 dBm, and High SFDR of 65.78dB, as illustrated in the Fig. 3a.

The conversion efficiency η for the configuration reported in [10], is the difference between the achieved intermediate signal power P_{IF} and message signal amplitude entered in the second modulator P_{RF}:

$$\eta = P_{IF} - P_{RF} = -10 - (-17.8) \text{ [dBm]} = 7.8 \text{ [dB]}. \tag{26}$$

When employing parameters for the proposed configuration we achieve an IF power amplitude of $P_{IF} = -4.28$[dBm],

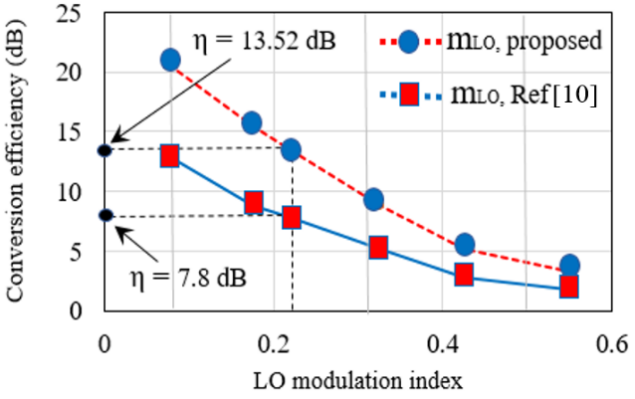

FIGURE 4. The conversion efficiency comparisons performed between integrated DPMZM and proposed DP-DPhM generating 80 MHz IF, by inverse biasing of both modulators as a function of LO modulation index.

with the highest spur of −75.84 dBm, and SFDR of 71.57dB, as illustrated in Fig. 3b. It should be noted that SFDR is referred to as a difference between IF peak power and highest spurs. In this study, we measured the IF bandwidth of 200 kHz.

For the same modulation indexes at the proposed configuration, calculated conversion efficiency is [18], [19]

$$\eta = P_{IF} - P_{RF} = -4.28 - (-17.8) \text{ [dBm]} = 13.52 \text{ [dB]}. \tag{27}$$

We have calculated conversion efficiency for numerous LO modulation indices values and constant RF input power values for both configurations. Based on the diagram illustrated in Fig. 1, when operating with a small LO modulation index, optical power entering the photodiode is smaller, which reduces the conversion efficiency.

The proposed configuration link is amplified using EDFA. The conversion efficiency rises much faster, but the photodiodes input power rises much slower, compared to the same system link without amplification Fig.1a.

This results in a low photodiodes input power and much higher conversion efficiency. As a point of comparison, configurations with dual-cascade [5] and DP-MZM based photonic mixers [10] are utilised.

By varying the LO modulation index m_{LO}, the highest downconverted signal strength has been achieved at the constant RF and lowest LO modulation indexes, as illustrated in Fig.4.

Our proposed structure configuration using VPI [17] simulation software confirms that, for the LO modulation index of $m_{LO} = 0.22$, we have managed to improve the conversion efficiency for 5.72 [dB] as compared to the configuration obtained by [10], and 28.4[dB] in contrast to the conventional dual-series modulator based photonic mixer, as illustrated in Fig. (4, 5).

The following step is calculating conversion efficiency for various RF frequency. In Fig. 6, we have shown measured conversion efficiency of DP-DPhM, as a function of various

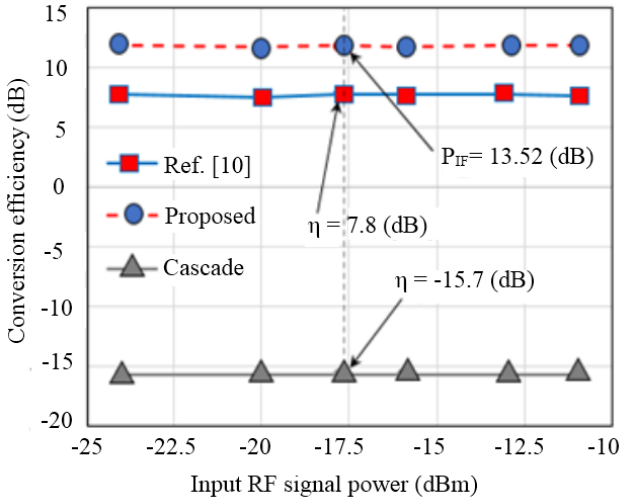

FIGURE 5. The DP-DDMZM based photonic downconverter conversion efficiency compared with the DP-MZM based photonic mixers [10], and conventional cascaded connected modulator, as function input RF signal power.

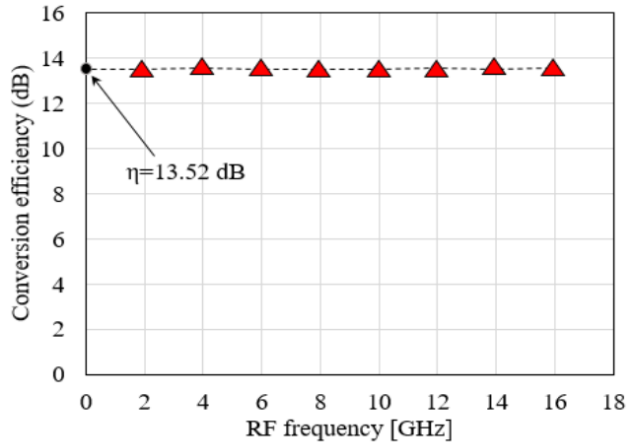

FIGURE 6. Conversion efficiency in function of RF frequency for the proposed DP-DPhM.

input RF signal frequency. To keep the IF signal frequency constant at the value of 80GHz, we must control the LO signal frequency in harmony to RF signal frequency [10].

As can be seen from Fig. 6, the achieved conversion efficiency for any RF frequency for the proposed configuration is generally a constant value of 13.52[dB], as shown in table 1.

When preparing the system link, SFDR is the most vital factor. To maximise the DR, the noise floor should be levelled to the distortion level. The SFDR for the downconverter, comparing proposed configuration with the configuration at the [10], is plotted in Fig. 7, [4].

The noise floor which is dominated by the shot noise and thermal noise is −162.87dBm/Hz.

From our simulation, for the modulation used at the [10], the SFDR is 115. 57[dB-Hz$^{2/3}$], and when using the proposed configuration SFDR is improved to 121.15[dB-Hz$^{2/3}$] [19].

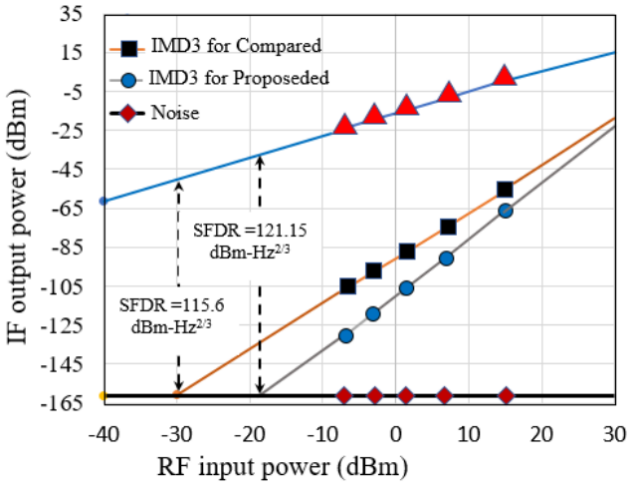

FIGURE 7. Downconverted IF signal and compared intermodulation distortion for both configuration in function of RF input power for the DP-DDMZM.

We have compared numerous simulations at various operating points. There is a slight difference between the transmission operating points as seen in table 2. If DD-MZM is designed to work as a phase modulator, the bias voltage must be set at the QTP where we will achieve constant conversion efficiency for any RF input power, as illustrated in the Fig. 5.

This will result in much higher conversion efficiency as compared to [10], as shown in table 2. The voltage applied to the electrical input of the MZM, such as modulating or bias, will change the refractive index and will lead to a phase shift between the message signal and carrier waves [16].

In this paper, we demonstrate the difference between the initial [10] structure and the proposed system configuration using DP-DPhM.

To achieve high conversion efficiency and SFDR, we have compared various input system parameters used at the DPMZM, such as the various input powers and the various bias voltages, working at various operating points [16].

The analytical calculations and simulation testing achieved at the RF side of the link are shown in table 2.

In table 2, we have listed the numerous SFDR results of the DPMZM, achieved at various operating points, with the link amplified or not amplified. To make both DPMZMs working as phase modulators, we should have a destructive recombination between the waves, which is a maximum decrease in the intensity at the output of the MZM.

As we have shown in table 2, with both our proposed configurations we have achieved higher SFDR, where link amplification (EDFA) plays a vital role. As compared to all the other conventional configurations, we have achieved higher intermediate signal power amplitude of $P_{IF} = -4.28$[dBm], and a minimum spur of −75.84[dBm] as shown in Fig.3b.

We have achieved a conversion efficiency of $\eta = P_{IF} - P_{RF} = -4.28-(-17.8) = 13.52$[dB]. This is a higher conversion efficiency compared to a conventional DPMZM based photonic mixer.

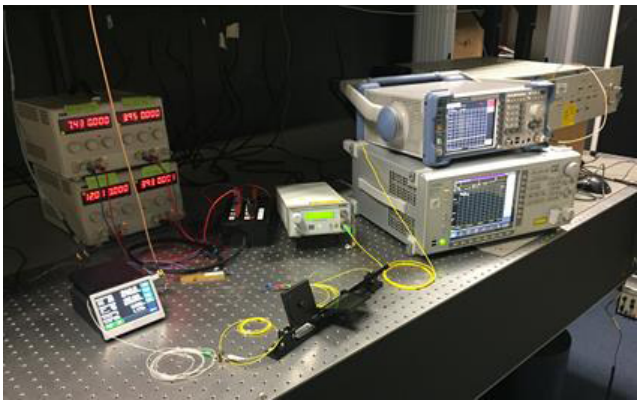

FIGURE 8. Proposed DPMZM based microwave photonic downconverter, at null operating point, push-pull drive mode, and gain added to the system by the EDFA. The experiment has been carried out in the Photonics and Optical Sensors (POS) Laboratory.

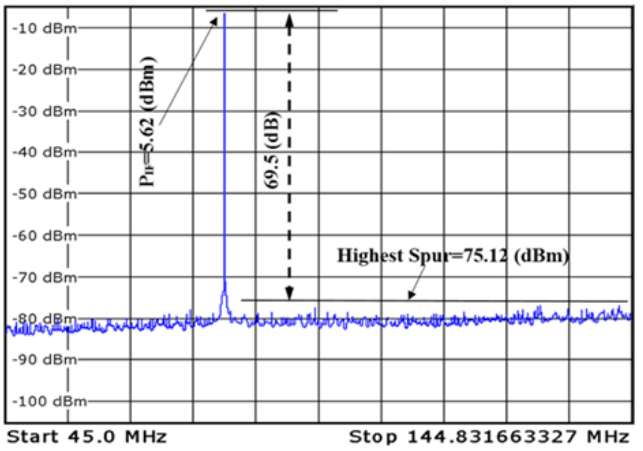

FIGURE 9. Experimentally measured output downconverted electrical spectrum (IF) of integrated DP-MZM based photonic mixer, for the proposed configuration.

VI. EXPERIMENTAL SETUP AND OBTAINED EXPERIMENTAL RESULTS

An experiment as a proof of concept has been demonstrated, based on the proposed mixer as illustrated in Fig. 2. An optical carrier of wavelength 1550nm at a power of 25mW is generated from CW laser. A Gallium Arsenide (GaAs) DPMZM of switching voltages 9.1V for parent modulator and a bandwidth of 25GHz is utilised. The first and second modulators of DPMZM have a switching voltage of 9.6V and 9.7V, respectively. A manual polarisation controller is utilised between a laser source and modulator to maintain the randomly generated light polarity. RF and LO signals are generated by signal generators. The modulators' voltages are controlled by a standard DC power supply source, using a modulator control box.

The optical output from the modulator is fed into a EDFA (EDFA100P) for the signal amplification. At the receiver, a PIN photodiode (DSC40S) of responsivity 0.8A/W with a RF amplifier (Microwave dB, DKM724302) is utilised. The IF signal is detected and analysed by an electrical spectrum analyzer. The developed experimental setup is shown in Fig. 8.

Based on the simulation results, to achieve high conversion efficiency, optical carrier has been suppressed. This has been achieved by using a tight control on the GaAs MZMs parameters, and minimum transmission operating at both modulators. To satisfy mathematical calculation and achieve maximum optical carrier suppression which is an 180° phase shift, both modulators are biased at NOP, and the parent modulator is biased at QTP realising 90° phase shifts and another 90° are realised from MMI embedded in the modulator.

The theoretical calculations achieved in section IV, for the LO modulation index $m_{LO} = 0.22$ and small RF modulation index value of $m_{RF} = 0.023$, were utilised and analysed in Section V through simulation analysis. Subsequently, the indices were utilised experimentally in section VI. A detailed analysis has been carried out resulting in the generated IF signal amplitude of 5.62dBm. Because of the limited experimental resources such connectors/adapters for the LO and RF, the LO and RF signal powers have dropped down less than 1dBm. This has resulted in the measured output downconverted electrical spectrum (IF), and in the ratio between the IF and highest spur which in this case is 69.5 dB, as illustrated in Fig. 9.

The experimentally achieved conversion efficiency for the proposed DP-DDMZM configuration is

$$\eta = P_{IF} - P_{RF} = -5.62 - (-18.3)\ [\text{dBm}] = 12.68\ [\text{dB}]. \tag{28}$$

The experimentally achieved IF amplitude that closely matches the simulation results, as shown in Fig. 3b, (Eq. (27)), is illustrated in Fig. 9, resulting in very close conversion efficiency illustrated using Eq. (28). This validates and reinforces the results achieved through simulation.

VII. CONCLUSION

We have developed a RoF analytical novel model and used VPI simulations where we have demonstrated a high downconversion structure with high efficiency, using two novel proposed configuration schemes. We have shown that the residual carrier has been cancelled by a combination of differential detection of two outputs, with inverse biasing of both modulators and to the second configuration by 180° phase shifting. The IF 'beat' term is realised within the 2x2 coupler mixer. We have benchmarked our developed simulation model with experimental work published by Ref. [10]. Comparisons have been performed for all conventional modulation schemes, at all transmission operating points.

High conversion efficiency has been achieved over a wide frequency range, with lower noise and high SFDR, with an improved conversion efficiency of 28.3 [dB] as compared to the conventional cascaded connected modulators and 5.72 [dB] as compared to previously published work using DP-MZM. To illustrate the link's conversion efficiency improvement, we have experimentally demonstrated the

RF downconversion. Our simulation analysis and experimentally obtained results match very well, which confirms that the proposed configurations would have significant impact on high-frequency links where downconversion is essential.

REFERENCES

[1] J. Yao, "Microwave photonics," *J. Lightw. Technol.*, vol 27, no. 3, pp. 314–335, Feb. 1, 2009.

[2] S. Merlo, M. Norgia, and V. Donati, "Fibre gyroscope principles," in *Handbook of Fibre Optic Sensing Technology*. Hoboken, NJ, USA: Wiley, 2000.

[3] A. K. M. Lam, M. Fairburn, and N. A. F. Jaeger, "Wide-band electrooptic intensity modulator frequency response measurement using an optical heterodyne down-conversion technique," *IEEE Trans. Microw. Theory Techn.*, vol. 54, no. 1, pp. 240–246, Jan. 2006.

[4] J. Luo, S. Li, X. Zheng, H. Zhang, and B. Zhou, "Highly linear W-band transmitter based on OFC and heterodyne up-conversion," in *Proc. 21st Optoelectron. Commun. Conf. (OECC) Held Jointly Int. Conf. Photon. Switching (PS)*, Niigata, Japan, 2016, pp. 1–3.

[5] G. K. Gopalakrishnan, W. K. Burns, and C. H. Bulmer, "Microwave optical mixing in LiNbO3 modulators," *IEEE Trans. Microw. Theory Techn.*, vol. 41, no. 12, pp. 2383–2391, Dec. 1993.

[6] H. Yu *et al.*, "Photonic downconversion and linearization of microwave signals from the *X* to *K*-band," *IEEE Photon. Technol. Lett.*, vol. 27, no. 19, pp. 2015–2018, Oct. 1, 2015.

[7] B. M. Haas and T. E. Murphy, "Linearized downconverting microwave photonic link using dual-wavelength phase modulation and optical filtering," *IEEE J. Photon.*, vol. 3, no. 1, pp. 1–12, Feb. 2011.

[8] J. Zhang, E. H. W. Chan, X. Wang, X. Feng, and B. Guan, "High conversion efficiency photonic microwave mixer with image rejection capability," *IEEE Photon. J.*, vol. 8, no. 4, Aug. 2016, Art. no. 3900411.

[9] T. R. Clark, S. R. O'Connor, and M. L. Dennis, "A phase-modulation I/Q-demodulation microwave-to-digital photonic link," *IEEE Trans. Microw. Theory Techn.*, vol. 58, no. 11, pp. 3039–3058, Nov. 2010.

[10] E. H. W. Chan and R. A. Minasian, "Microwave photonic downconverter with high conversion efficiency," *J. Lightw. Technol.*, vol. 30, no. 23, pp. 3580–3585, Dec. 1, 2012.

[11] R. G. Walker, M. F. O'Keefe, N. Cameron, H. Ereifej, and T. Brast, "Gallium arsenide electro-optic modulators," in *Proc. IEEE Compound Semiconductor Integr. Circuit Symp. (CSICS)*, La Jolla, CA, USA, Oct. 2014, pp. 1–4.

[12] R. G. Walker, N. I. Cameron, Y. Zhou, and S. J. Clements, "Optimized gallium arsenide modulators for advanced modulation formats," *IEEE J. Sel. Topics Quantum Electron.*, vol. 19, no. 6, pp. 138–149, Dec. 2013.

[13] R. A. Griffin *et al.*, "10 Gb/s optical differential quadrature phase shift key (DQPSK) transmission using GaAs/AlGaAs integration," in *Proc. Opt. Fiber Commun. Conf. Exhib.*, 2002, pp. FD6-1–FD6-3.

[14] B. Chen, S. L. Zheng, X. M. Zhang, X. F. Jin, and H. Chi, "Simultaneously realizing PM-IM conversion and efficiency improvement of fiber-optic links using FBG," *J. Electromagn. Waves Appl.*, vol. 23, pp. 161–170, Jan. 2009.

[15] S. Shimotsu *et al.*, "Single side-band modulation performance of a $LiNbO_3$ integrated modulator consisting of four-phase modulator waveguides," *IEEE Photon. Technol. Lett.*, vol. 13, no. 4, pp. 364–366, Apr. 2001.

[16] Y. Li, Y. Zhang, and Y. Huang, "Any bias point control technique for Mach-Zehnder modulator," *IEEE Photon. Technol. Lett.*, vol. 25, no. 24, pp. 2412–2415, Dec. 15, 2013.

[17] *VPIphotonics*. Accessed: Jun. 2017. [Online]. Available: http://www.vpiphotonics.com/index.php

[18] P. Li, W. Pan, X. Zou, S. Pan, B. Luo, and L. Yan, "High-efficiency photonic microwave downconversion with full-frequency-range coverage," *IEEE Photon. J.*, vol. 7, no. 4, pp. 1–7, Aug. 2015.

[19] P. Li, W. Pan, X. Zou, B. Lu, L. Yan, and B. Luo, "Image-free microwave photonic down-conversion approach for fiber-optic antenna remoting," *IEEE J. Quantum Electron.*, vol. 53, no. 4, May 2017, Art. no. 9100208.

[20] C. T. Lin, J. Chen, S. P. Dai, P. C. Peng, and S. Chi, "Impact of nonlinear transfer function and imperfect splitting ratio of MZM on optical up-conversion employing double sideband with carrier suppression modulation," *J. Lightw. Technol.*, vol. 26, no. 15, pp. 2449–2459, Aug. 2008.

[21] M. Chtioui *et al.*, "High responsivity and high power UTC and MUTC GaInAs-InP photodiodes," *IEEE Photon. Technol. Lett.*, vol. 24, no. 4, pp. 318–320, Feb. 15, 2012.

FADIL PALOI received the B.S. and M.S. degrees in electric engineering from the University of Prishtina, Kosovo, in 1987, and the M.S. degree in power system and energy management from the City, University of London in 2011. He is currently pursuing the Ph.D. degree in fiber optic signal transmission with the University of Bedfordshire, U.K., with a focus on multi user optical signal transmission and utilizing SSB modulation. His research interests include the key aspects of long-haul signal transmission, analyses, and essential issues related to the modulation and dispersion compensation.

SHYQYRI HAXHA (SM'14) received the M.Sc. and Ph.D. degrees from the City University of London in 2000 and 2004, respectively, and several world-class industrial E.M.B.A. and M.B.A. diplomas. He was a Lecturer in optic communication with the Electronics Department, Kent University, Canterbury, U.K. He was a Reader in photonics with the Computer Science and Technology, University of Bedfordshire, Luton, U.K. He is currently a Reader in electronic engineering with the Department of Electronic Engineering Egham, Royal Holloway, University of London, U.K. He has also research expertise on photonic crystal devices, metamaterials, biosensors, photonic crystal fibers, geometrical optics, surface plasmon polaritons, ultra-high-speed electro-optic modulators, optical CDMA, and optical MIMO systems. His current research interests include microwave photonics, RF transmission over fiber optics, and designing and demonstrating optical sensors for personal health monitoring and environmental applications. In 2003, he received the SIM Postgraduate Award from The Worshipful Company of Scientific Instrument Makers, Cambridge, U.K., for his highly successful contribution in research.

Dr. Haxha has extensive expertise in Telecommunication Management Industry. He was a Telecommunication CEO in partnership with Cable & Wireless Communications Ltd., a British multinational telecommunications company, and Monaco Telecom International. He is an Associate Editor of the IEEE Sensors Journal. He has been a keynote speaker of numerous world class conferences.

TAIMUR N MIRZA received the B.Eng. degree (Hons.) in electrical and electronics engineering and the M.Sc. degree in embedded intelligent systems from the University of Hertfordshire, U.K., in 2013 and 2014, respectively. He is currently pursuing the Ph.D. degree in transmission of microwave signals over fiber optics communication systems with a prime focus on the compensation and suppression of nonlinearly generated harmonics. His research interests include the long-haul transmission in the radio-over fiber system.

MOHAMMED SHAH ALOM received the B.Eng. degree (Hons.) in telecommunication and network engineering from the University of Bedfordshire, U.K., in 2013. He is currently pursuing the Ph.D. degree in microwave photonic signal processing funded by Leonardo defense and security systems. He was an Engineering Laboratory Demonstrator with the University of Bedfordshire from 2013 to 2016, where he contributed to many engineering research project. His research interests include mainly microwave photonic signal processing, digital signal processing, and embedded systems.